Erosion Potential and Water Quality Impacts: Big Dry Creek, CO

Final Report

By:

Roderick W. Lammers
Colorado State University

Brian P. Bledsoe
University of Georgia

Image of Big Dry Creek courtesy of THK Associates

EXECUTIVE SUMMARY

Big Dry Creek is experiencing channel instability, caused primarily by alteration to the watershed's hydrology and sediment dynamics. Using field and GIS-based analyses, we summarize the current geomorphic status of Big Dry Creek, identify areas prone to future erosion, and provide some recommendations to reduce channel instability and improve stream health, in terms of both aquatic habitat and water quality.

Big Dry Creek is subject to both channel incision (erosion of the bed) and bank erosion. Currently, however, the channel is relatively vertically stable and is adjusting primarily through meander bend migration. Historically, this lateral erosion has contributed a small portion of the total phosphorus load but most of the suspended sediment load measured at the watershed outlet. We used bank stability data collected in the field to develop an equation to estimate probability of failure for all channel banks. These data can be used to identify areas where banks are prone to failure and where bank stabilization may be warranted. Finally, we identified erosion and deposition-dominated reaches using stream power as a surrogate for sediment transport capacity. This analysis showed local erosion is usually balanced by deposition but that the channel still has significant excess transport capacity – and is therefore still erosion prone.

Based on these analyses, we make several recommendations for mitigating future channel instability in Big Dry Creek:

- **Flow management**: Excess erosion is primarily caused by larger, longer, and more frequent discharges. Stormwater controls that reduce peak flow magnitude and the duration that high flows exceed erosion thresholds will improve channel stability.
- **Floodplain reconnection:** Reconnecting the stream to its floodplain will dissipate the energy of large discharges, reducing their erosive power.
- **Grade control:** Although much of the channel appears relatively vertically stable, there is the potential for continued incision. Targeted grade control structures will guard against additional bed degradation.
- **Bank stabilization/revegetation:** The GIS bank stability analysis identified areas with unstable banks that may benefit from bank stabilization, including revegetation.
- **Monitoring and future analysis:** Continued monitoring is essential to identify ensure mitigation strategies are working and identify any new areas of instability.

INTRODUCTION

This report summarizes historic and current channel stability for Big Dry Creek. Its purpose is to analyze the extent to which erosion in Big Dry Creek influences water quality (e.g. phosphorus and suspended sediment loading) and assess future susceptibility to erosion. To meet these goals, we conducted several analyses:

1. Collected field data on bank stability and bank phosphorus content.
2. Analyzed historic erosion rates using satellite images and calculated phosphorus and suspended sediment loading as a result of this erosion.
3. Used a digital elevation model to estimate bank heights and angles along the channel and computed probability of failure for each of these banks.
4. Used differences in cumulative stream power as a metric for sediment transport capacity to identify erosional and depositional areas along Big Dry Creek.

The results from these analyses can be used to identify potential areas for stream rehabilitation to reduce channel erosion. By assessing the watershed as a whole, this report can help inform sustainable and integrative watershed planning that can lead to a more resilient Big Dry Creek.

Current Geomorphic Conditions

As is the case for many Front Range streams, the hydrology of Big Dry Creek has been significantly altered over time. Over 100 years ago, Standley Lake was constructed in the upper watershed to store water for agricultural and municipal uses, with highly managed water releases still occurring to meet the needs of downstream users. Additionally, land use changes affect stormwater runoff, irrigation practices affect diversions and return flows, and wastewater treatment plant discharges occur at several locations. Furthermore, water is imported from other basins to meet water demands. In response to this alteration, the channel has undergone a series of changes. First, there has been widespread incision, or channel bed erosion, which has created a deeper, more confined channel. However, incision has slowed or halted in many areas due to a number of artificial and natural grade controls which are relatively resistant to further erosion. These include unintentional grade controls such as bridges and culverts as well as structures designed specifically to prevent further erosion. Additionally, in some places the channel has eroded through its alluvium and encountered a naturally occurring clay layer which is more resistant to erosion than the sand/fine gravel bed material. As the bed has become more erosion resistant, the channel has begun to adjust primarily through bank erosion and lateral migration.

Bank erosion is occurring through two primary mechanisms, fluvial erosion and mass wasting. High flows are contained within the incised channel rather than accessing the floodplain. This has increased the erosive power of these flows and resulted in fluvial erosion of the channel banks. As the banks become steeper and taller as a result of this erosion, they become unstable and collapse (mass wasting) contributing large blocks of soil into the channel. This bank erosion has resulted in channel widening (equal erosion on both banks) and lateral migration of meander bends (greater erosion on one bank). This continued erosion contributes significant loads of sediment to the stream. Much of this sediment is being deposited in the lower reaches of Big Dry Creek (near its confluence with the South Platte). In other areas, however, there is no evidence of significant deposition, suggesting that there is still excess sediment transport capacity and that erosion will continue until the channel has adjusted (by

widening and/or reducing its slope) such that the transport capacity matches the sediment supply. The time scale for this adjustment is unknown due to a number of factors. First, continued urbanization in the watershed may further disturb the hydrology which would initiate further channel changes. Second, increases or decreases in the upstream sediment supply (either from channel erosion or out of channel sources) could either hasten or delay the return of the channel to a quasi-equilibrium state.

Channel Evolution Model

To help describe how stream channels change in response to disturbance, river scientists have developed numerous Channel Evolution Models (CEM). These CEMs describe the evolution of a stream channel as a series of stages (Figure 1). In Stage I, the channel is in its initial, undisturbed state. Some change to the hydrology (e.g. urbanization increasing flows) or sediment supply (e.g. urbanization decreasing sediment supply) creates an imbalance in the stream. Initially, the channel incises (e.g. bed erodes), creating steeper, taller banks (Stage II). As this incision continues, the banks become unstable and collapse, causing the stream to widen (Stage III). Eventually, the stream widens and incises enough that its ability to transport sediment is less than its sediment supply, causing deposition in the channel (Stage IV). Finally, this deposited sediment is stabilized by vegetation and a new, inset floodplain is formed (Stage V). The stream is now relatively stable but is confined within its former banks. This sequence of erosion may be initiated again by additional changes to the stream's hydrology and/or sediment supply.

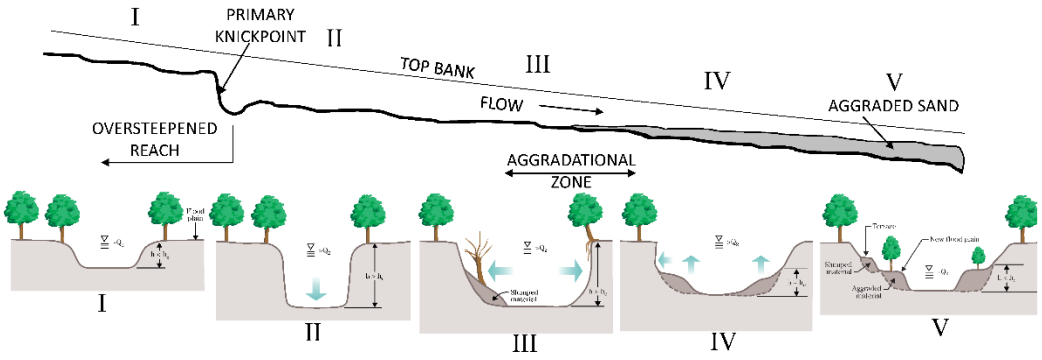

Figure 1. Channel evolution model. An initially stable channel (I) is disturbed, leading to incision (II). As banks become taller and steeper, they collapse, causing rapid widening (III). Eventually, the channel slope is reduced enough that sediment is deposited (IV) and the channel re-stabilizes (V). This sequence also occurs longitudinally throughout a watershed, with upstream migration of a knickpoint and channel erosion which supplies high loads of sediment to downstream reaches where it is deposited. Adapted from Schumm et al. (1984) and NRCS (2007).

METHODS

Field Data Collection

During summer 2015, we collected field data at 24 sites along Big Dry Creek. Prior to the field campaign, we divided the channel into eight reaches that had relatively homogenous land use and riparian condition. We also attempted to separate reaches at major grade controls (e.g.

road crossings, diversion structures, or bed stabilization structures). We sampled three sites within each of the eight reaches. We measured bank height, bank angle, and channel slope. We also collected soil samples from two banks per site which we analyzed for phosphorus content and soil texture. Finally, we qualitatively assessed riparian condition, percent of banks failing, bed material, and CEM stage.

Satellite Imagery Analysis

We used historic and current satellite imagery of the Big Dry Creek watershed from Google Earth to quantify historic bank erosion. We digitized stream bank lines for both 1993 (June) and 2014 (October) imagery. Channel polygons for 1993 and 2014 were constructed in ArcMap. Eroded area polygons were then constructed based on channel changes between these two years. These eroded area polygons were shrunk by 2 m on all sides to provide a more conservative estimate of eroded area, accounting for errors in the digitization process. Volumetric loading rates were determined by multiplying areal loading rates by adjacent bank heights obtained from the GIS analysis (see following section).

Bulk density data were collected from the USDA soil survey for the soils adjacent to the stream. This yielded 34 data points that followed a triangular distribution. Bank phosphorus data were obtained from laboratory analysis of field-collected bank soil (see Appendix for full dataset). Total phosphorus followed a normal distribution. Soil density and bank phosphorus concentrations were used to calculate mass phosphorus loading rates for each eroded polygon. The average annual loading rate from the basin was then calculated by dividing by the time period between aerial photographs (~21.3 years). We used a Monte Carlo simulation (repeating these calculations 10,000 times with ranges of input values) to produce a probability distribution of loading rates which accounts for uncertainty in the calculations. We conducted a similar analysis to calculate suspended sediment contribution from bank erosion. We multiplied the mass loading rates by the percentage of silt and clay in the bank material (varied from 40-60% in collected soil samples).

Bank Stability and GIS Analysis

Bank stability is primarily controlled by bank height, angle, and soil strength. If we assume soil strength is relatively consistent along Big Dry Creek, we can predict bank stability based only on bank height and angle using logistic regression. Logistic regression is useful for cases when the response variable is binary (e.g. 0 or 1, yes or no). In this case, the binary response variable is bank stability (i.e. stable or unstable). However, rather than simply predicting this binary response, logistic regression models the probability of response over a continuous range of 0 to 1. This allows for estimates of bank stability thresholds but also quantifies probability of failure rather than a simple stable/unstable classification. Logistic regression models the probability of a response (p) given a set of one or more independent variables (x_i):

$$p = \frac{\exp(\beta_o + \beta_1 x_1 + \cdots + \beta_n x_n)}{1 + \exp(\beta_o + \beta_1 x_1 + \cdots + \beta_n x_n)} \quad (1)$$

We can rearrange this equation to give the log-odds of bank failure for given bank height and angle:

$$\ln\left(\frac{p}{1-p}\right) = \beta_o + \beta_\alpha \ln \alpha + \beta_H \ln H \quad (2)$$

Where the β values are fitted model coefficients, α is angle (degrees), and H is height (meters).

Using bank geometry data for all reaches along Big Dry Creek, we fit the logistic regression model using the R statistical software package (version 3.4.0). Bank stability curves can be constructed based on the logistic regression results by assuming a value of p (e.g. 0.5 = 50% risk of failure). This gives an exponential relationship between bank height and angle which can be plotted with field data to visualize the threshold between stable and unstable banks (as well as the uncertainty associated with this threshold).

This logistic regression equation can be used with remotely sensed bank heights and angles to predict bank stability along the entire length of Big Dry Creek. We used a high resolution (0.75 m x 0.75 m grid cells) Digital Elevation Model (DEM) developed using LiDAR data collected after the September 2013 flood (data from Colorado GeoData Cache - https://geodata.co.gov/). We used GIS tools generously provided by Biron et al. (2013) to delineate the river channel, resulting in lines along each bank toe. Each bank line was buffered 7.5 m away from the channel to cover the entire bank. We calculated the bank height and slope in each bank "polygon" and stored these values in points spaced every 5 m along the right and left banks. Given these values, we used the logistic regression equation developed above (Eq. 1) to calculate the probability of failure for each of the banks.

Stream Power Mapping

Stream power is a measure of the energy available to do work in a stream. It is a relatively simple variable to calculate using discharge, channel slope, and channel width:

$$\omega = \frac{\gamma Q S}{w} \qquad (3)$$

Where ω is specific stream power (W/m^2), γ is the specific weight of water (9810 N/m^3), Q is discharge (m^3/s), S is slope (m/m), and w is width (m). Channel slope and width can be computed throughout a stream network using high resolution DEMs. Discharge can be obtained from gaging stations and scaled through the entire stream network based on drainage area. This allows stream power to be easily computed for entire watersheds – enabling large scale analysis of erosion and deposition trends. We used the Biron et al. (2013) GIS tools to extract channel slope and width along the entire length of Big Dry Creek.

We calculated daily flow rates at each of these points using USGS gage data from both the upstream (gage 06720820) and downstream (gage 06720990) gages. We accounted for water inputs from Standley Lake (summer only), Walnut Creek, and the Broomfield and Westminster wastewater treatment plants and water withdrawals from five major ditches along the channel (summer only). Discharge from the Northglenn wastewater plant was not included because it is a relatively minor contributor (although it has increased some in recent years). Using these discharge, slope, and width values we calculated cumulative stream power (power summed across the entire available flow record) at 10 m increments along the channel. We only used dates when both gages had flow data. The cumulative stream power is therefore summed over ~24.6 years of flow data (Oct 1991 – June 2017, omitting Oct 1995 – Oct 1996 where the upstream gage had no data).

Absolute stream power is informative but the *difference* in stream power between adjacent reaches is most useful for determining deposition or erosion potential. A reach with high stream power directly downstream from an area of low stream power will be prone to erosion because

sediment inputs will presumably be less than the transport capacity of the reach. On the other hand, a low power reach downstream from a high power reach will be deposition-dominated because it has low transport capacity compared to its upstream neighbor. A sequence of reaches with relatively similar stream power can be considered “transport” reaches because capacity-supply should be in balance and no net deposition or erosion will occur. We calculated differences in stream power for each point and the average of the 100 m reach immediately upstream to assess erosion and deposition potential along the entire stream length.

RESULTS

Field Data Collection

Map 1 shows the locations of the field sites, colored by reach. Example photographs from all reaches are attached to this report. Changes in channel form and erosion magnitude can be clearly seen moving downstream. In general, the upper reaches (1 – 4) are more vertically stable, although there is still significant bank erosion, especially on the outside of meander bends. The upper three reaches have substantial gravel and coarser material on their beds. By reach 4, the channel bed is nearly entirely sand with isolated areas of exposed clay. The field reconnaissance suggests that the percentage of failing banks increases moving downstream (Figure 2). These observations also indicate that the upper reaches of the stream are generally in the later stages of the CEM (Stage IV-V), as evidenced by sediment deposition within in the channel and the formation of inset floodplains in some areas. The lower reaches (5 – 8) are generally in the earlier stages of the CEM (Stage II-III) – although these reaches might be classified as in a state of “arrested incision”. Here, the channel has incised and there has been some widening and bank erosion; however, natural and artificial grade controls appear to be limiting further incision. This may prevent widespread bank instability and significant widening. The larger percentage of bank failures in these lower reaches is primarily from smaller, more frequent failures rather than the tall, eroding cutbanks observed in some of the upper reaches (see, for example, Photos 5, 6, and 8).

Satellite Imagery Analysis

Figure 3 shows an example of calculated eroded areas from the satellite imagery analysis. This analysis suggests that this source accounts for an average of ~10% of the total annual phosphorus load in Big Dry Creek (Figure 4). Although it is not a major contributor, bank erosion is still a measurable source of phosphorus in this watershed. On the other hand, our analysis suggests that bank erosion accounts for essentially all of the suspended sediment supplied to the stream (Figure 5). This analysis doesn’t account for sediment deposition and storage in the channel and floodplain and may be an overestimate.

While bank erosion is not the primary source of phosphorus loading to Big Dry Creek, it is a major contributor of suspended sediment. Based on long-term monitoring by the Big Dry Creek Watershed Association, the primary source of phosphorus loading is municipal wastewater treatment plant discharges, although recent plant upgrades have significantly reduced phosphorus loading (see the significant drop in total phosphorus loading post 2009 in Figure 4). This drop in the total watershed phosphorus load means a larger percentage of this load may be attributed to bank erosion. Bank stabilization can reduce both phosphorus and sediment inputs to the stream, but will be insufficient for addressing phosphorus pollution without reducing loading from other sources.

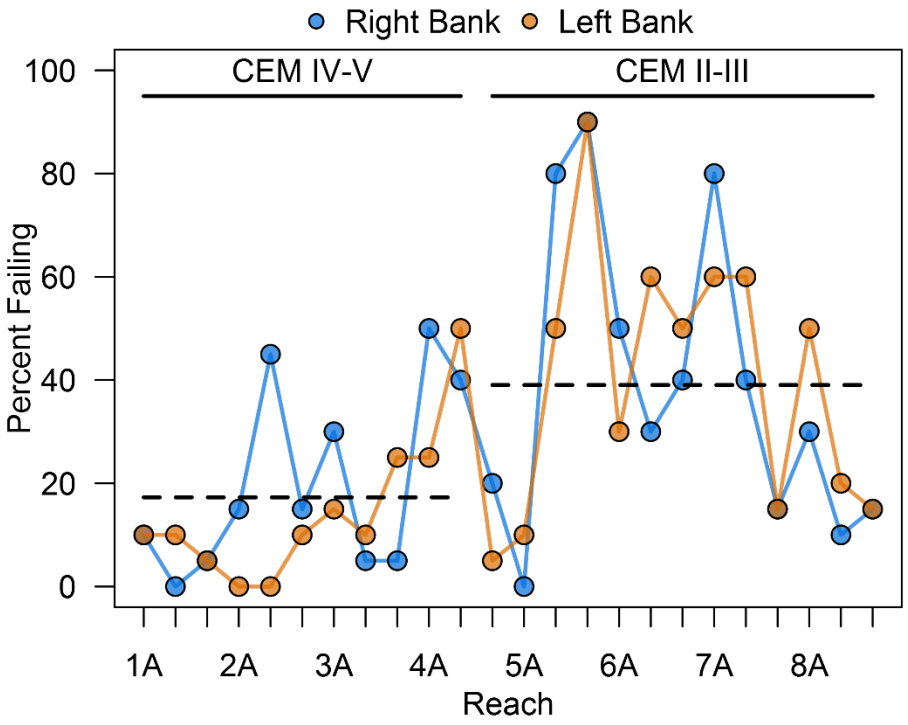

Figure 2. Field estimates of the percentage of right and left banks failing for each site. The upstream section (Reach 1A – 4B) was in CEM stage IV-V (stabilizing) while the downstream section (Reach 4C – 8C) was in CEM stage II-III (incising and widening). Horizontal dashed lines are the mean percent of banks failing for each group.

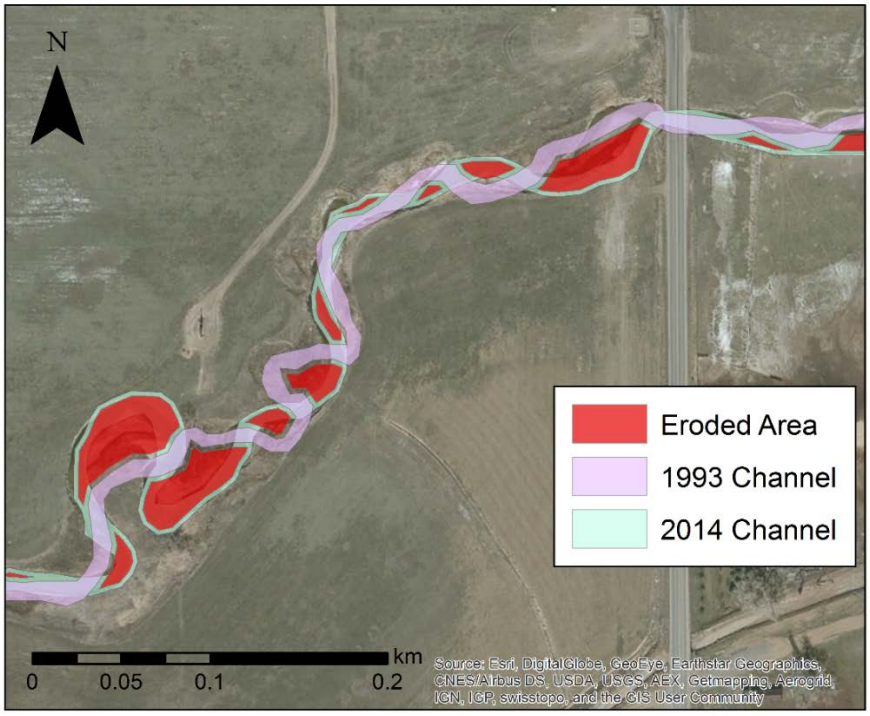

Figure 3. Example map of the satellite imagery analysis showing the 1993 and 2014 digitized stream channels. Red polygons are the areas eroded from channel migration over this time period.

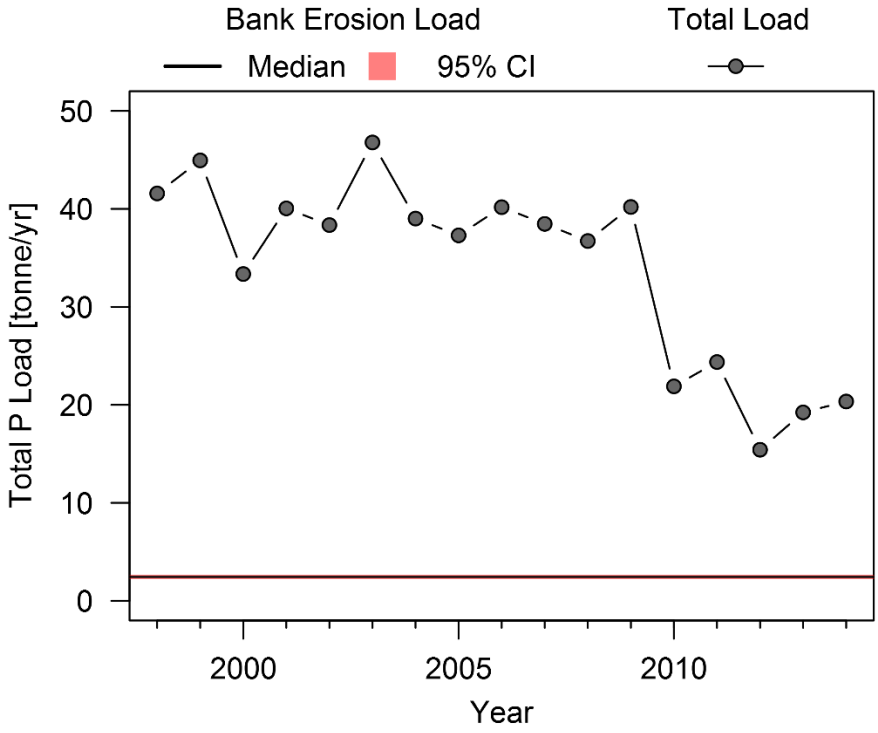

Figure 4. Calculated total phosphorus load (metric tonnes / year) from bank erosion (with shaded 95% confidence interval) compared to the total annual phosphorus load measured at the outlet of Big Dry Creek. Note the 95% CI is very narrow and may be difficult to see.

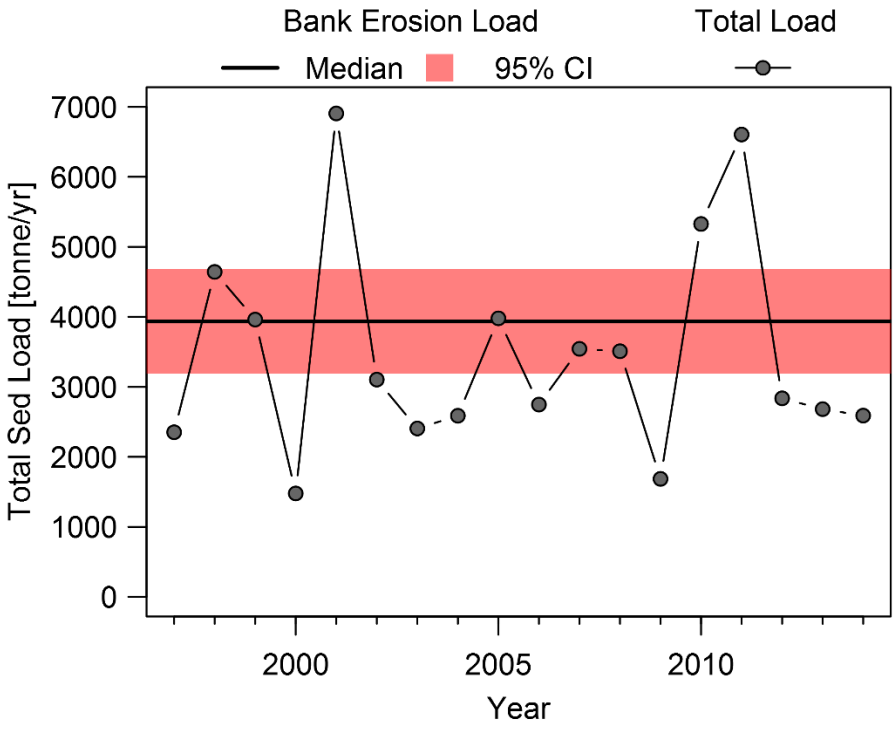

Figure 5. Calculated total suspended sediment load (metric tonnes / year) from bank erosion (with shaded 95% confidence interval) compared to the total annual suspended sediment load measured at the outlet of Big Dry Creek.

Bank Stability and GIS Analysis

Figure 6 shows bank heights and angles from stable and unstable banks. Curves are the fitted logistic regression model ($\beta_o = 27.1,\ \beta_\alpha = -6.5,\ \beta_H = -3.4$) for different failure probabilities. There is some overlap between unstable and stable banks which suggests that our assumption of consistent bank strength was not entirely accurate. This uncertainty, however, is incorporated within the logistic regression model (i.e. the distance between the 10% and 90% lines).

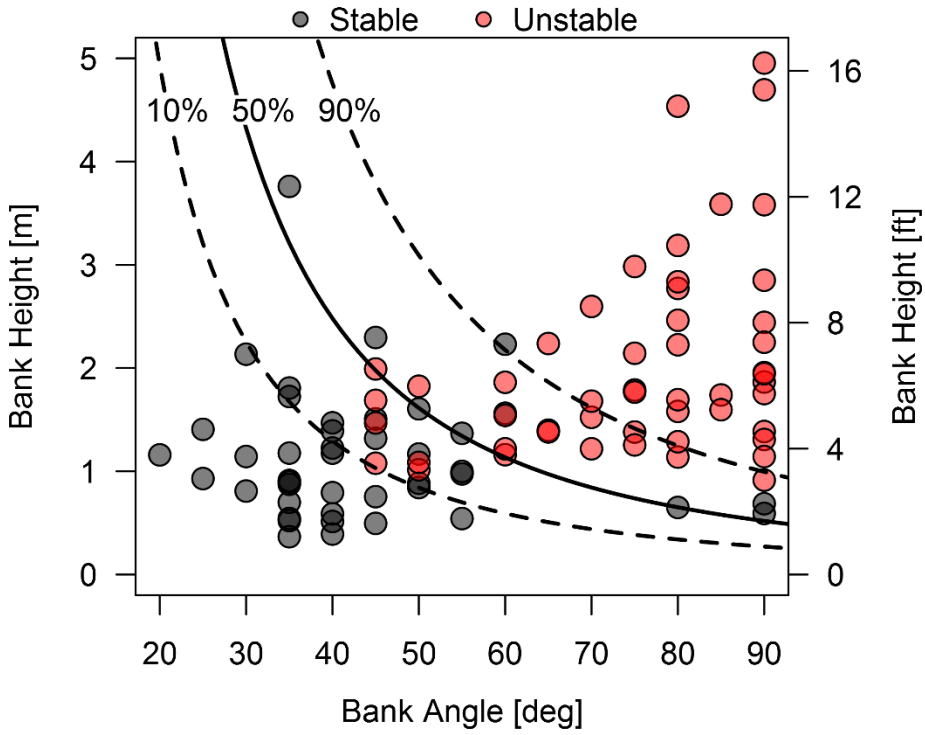

Figure 6. Field collected data on bank height and angle for stable and unstable banks. Lines show probabilities of failure predicted from the logistic regression equation.

Figure 7 compares our field measured bank heights and angles with those obtained from the GIS analysis. Our GIS approach did a relatively good job of predicting bank heights but it consistently under-predicted bank angles. While the DEM is relatively high resolution (0.75 x 0.75 m), it still is insufficient to capture very steep (>70 degree) slopes, especially on relatively short banks. The points in Figure 7b are sized relative to bank height (large = taller banks). Bank angles were somewhat more accurate for the taller banks where elevation and slope differences were better captured by the DEM.

Because our GIS approach underpredicted bank angles, our bank stability analysis is conservative (i.e. generally predicts banks are more stable than they might be). However, it is still useful for identifying areas with unstable banks where restoration actions might be warranted. Probability of failure for both right and left banks are shown in Maps 2-3. For both banks, most of the failure prone areas are in the upper half of the watershed. Although this portion of the channel is in the latter stages of the CEM and is not experiencing further incision, banks are generally taller than downstream and still show signs of failure and lateral migration. Figure 8 is a zoomed-in view of a single stretch of channel with both right and left bank failure

probabilities. The unstable banks are clearly located on the outside of meander bends. This is common throughout Big Dry Creek where bank erosion is mostly on one bank or the other, suggesting that the channel is adjusting primarily by lateral migration rather than significant widening. This is partially confirmed by comparing channel width and sinuosity between 2014 and 1993 using the results of the aerial imagery analysis (Figure 9). These data indicate a mix of channel widening and narrowing, but the small average width change is not statistically different from zero (Wilcox signed rank test). Sinuosity, on the other hand, does show a statistically significant increase from 1993 – 2014 (average increase of 0.052). This analysis omits a large meander cutoff which decreased channel sinuosity in one reach by ~1.6 (incorporating this data point still resulted in a statistically significant increase in sinuosity).

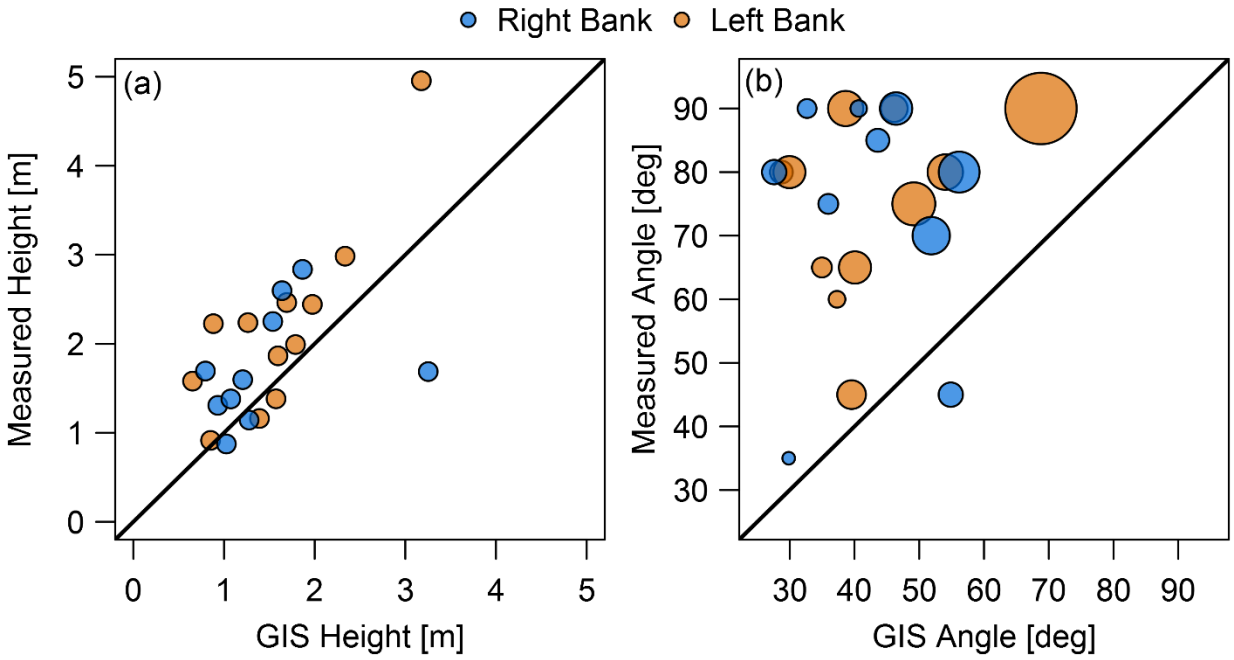

Figure 7. Field measured heights (a) and angles (b) versus values obtained from the high resolution DEM. Dots are colored based on location (right or left bank). Points in the angle plot (b) are sized according to bank height (e.g. larger points for taller banks).

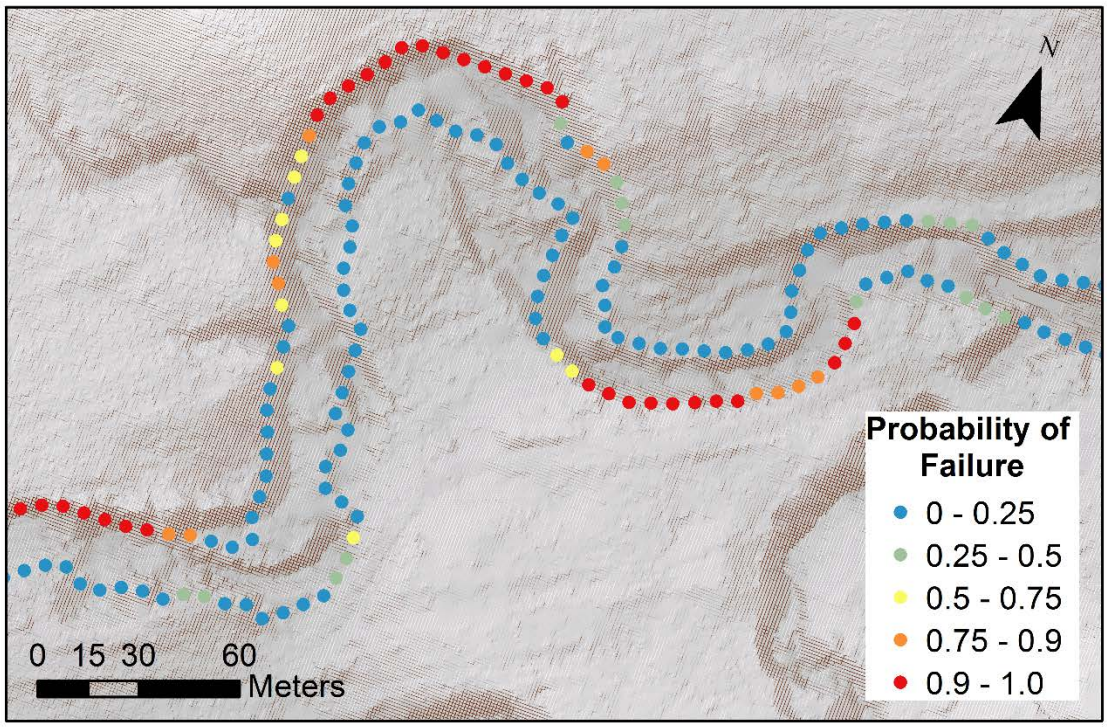

Figure 8. Example map showing the probability of bank failure calculated from the logistic regression equation. High resolution DEM is shown in the background. Flow direction is left to right.

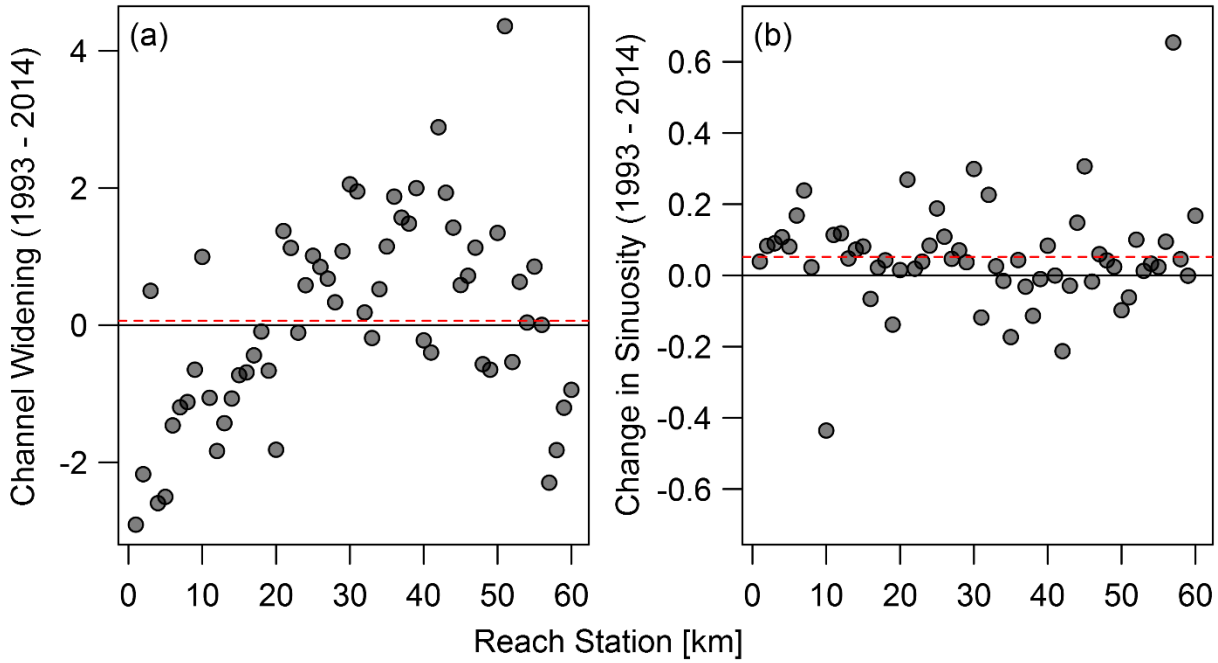

Figure 9. Changes in channel width (a) and sinuosity (b) from 1993 – 2014 for the same 60, ~1 km reaches. Dashed red lines are mean values.

Stream Power Mapping

Maps 4a-b show differences in cumulative stream power along Big Dry Creek. There is a mix of deposition- and erosion-dominated sections, but the majority of the channel is classified as "transport" (i.e. no net erosion or deposition). There are no apparent trends in erosion or deposition potential. Most erosion-dominated points appear to be balanced by an adjacent depositional area (and vice versa). This can also be seen by plotting stream power difference by downstream distance (Figure 10). This suggests qualitatively that local erosion in Big Dry Creek is relatively balanced by local deposition. Quantitatively, however, we can see that the magnitude of the erosion areas (positive values) are much larger than the magnitude of depositional areas (negative values). In fact, the sum of the stream power difference values along Big Dry Creek is ~230 kW/m which indicates that there is significant excess power in the stream and it is overall erosional.

Many of these erosion-deposition sequences are located at bridge crossings, diversions, or grade control structures. For example, the largest peak, just upstream from 120th Ave, is a grade control structure co-located with the upstream USGS gage. These areas tend to be artificially armored to prevent significant erosion so many of the erosional and depositional areas identified in this analysis may be in parts of the channel that are less inherently prone to change. There are other areas, however, which may not be armored and are therefore susceptible to erosion. Figure 11 is a zoomed-in view of a single reach showing the results of the stream power difference analysis. The sequence of erosion, deposition, and transport-dominated reaches can be clearly seen moving downstream.

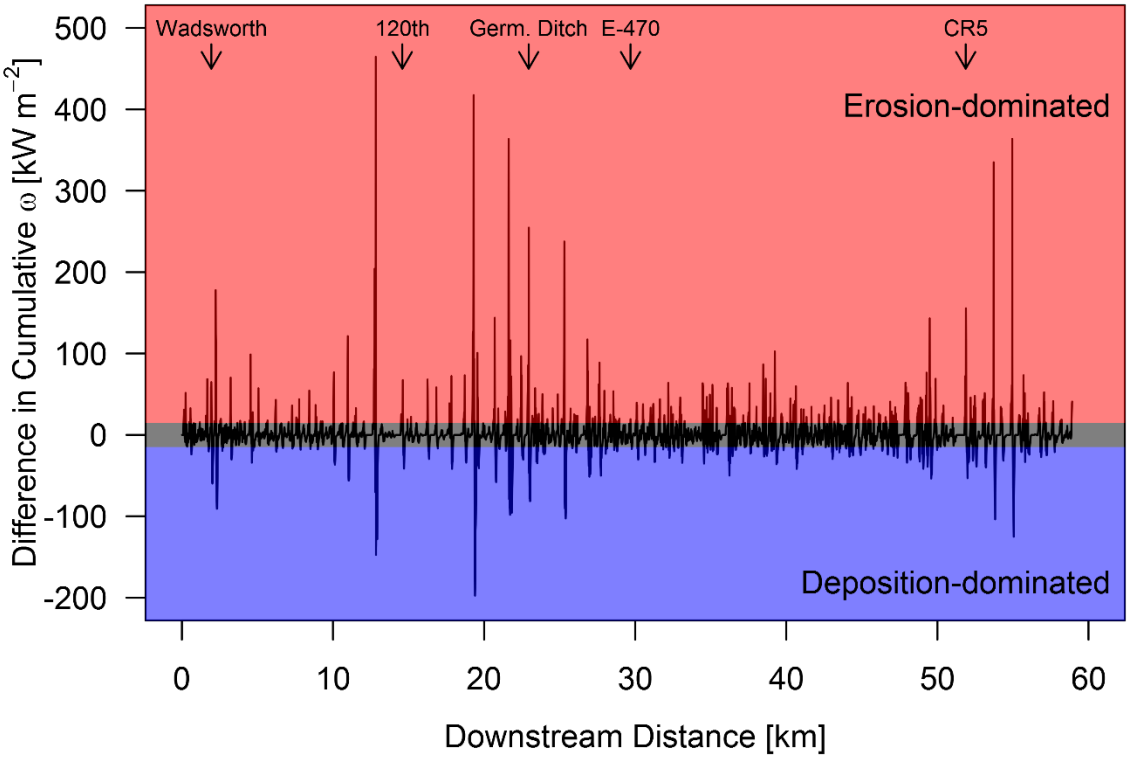

Figure 10. Difference in cumulative stream power versus downstream distance. Gray shaded band is ± 15 kW/m^2, an approximate threshold for transport-dominated reaches. Locations of various road crossings and one diversion are identified by arrows.

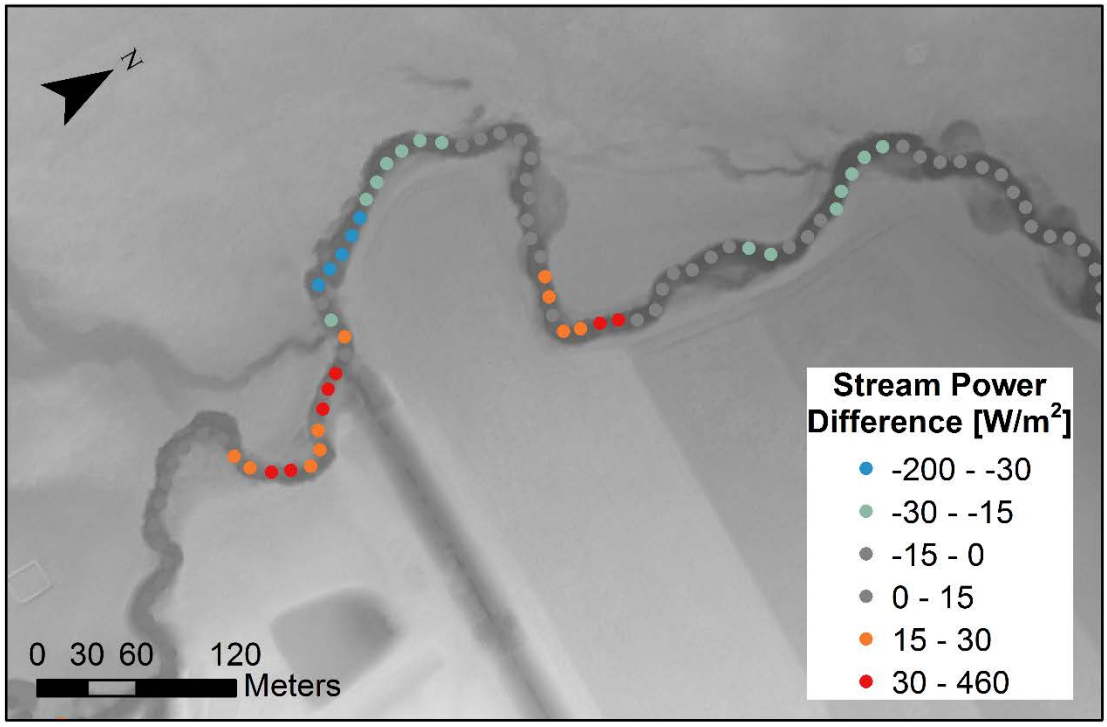

Figure 11. Example map of the stream power difference analysis. Red and orange regions are erosion-dominated, blue and green are deposition-dominated, and gray are transport-dominated. High resolution DEM shown in background. Flow direction is left to right.

CONCLUSIONS AND RECOMMENDATIONS

The field reconnaissance and GIS analysis allows us to make some general conclusions about the current state of Big Dry Creek and potential trajectories of channel change. The entire length of the channel has incised, although the magnitude of incision tends to decrease moving downstream. Many of the upper reaches (1-4) have a relatively stable bed and do not appear prone to significant future incision. The lower watershed has incised less, and in many places the channel has encountered a stiff clay layer which is resistant to erosion and should slow further bed degradation. The channel here may be considered in a state of “arrested incision” where bank heights have not increased enough to become widely unstable.

Despite the relative stability of the channel bed, Big Dry Creek is still laterally unstable and is prone to meander bend migration. This is supported by a measured increase in sinuosity from 1993 – 2014 (Figure 9) and the fact that most unstable banks are located on the outside of bends (e.g. Figure 8). This lateral migration is relatively consistent throughout the watershed; however, bank heights are generally higher in the upper watershed because this area has experienced more incision. These banks are more susceptible to failure and will contribute larger volumes of sediment and phosphorus to the channel than the smaller banks in the lower watershed.

Big Dry Creek's altered hydrology is the most likely cause of continued channel erosion. Urbanization and irrigation releases from Standley Lake have increased flow flashiness (how quickly water levels rise and fall) and flow magnitudes. These high flows are contained within the incised channel and cannot dissipate their energy on the floodplain. This frequent erosion maintains steep, tall banks which are then more prone to failure. Additionally, wetting and drying cycles caused by rising and falling water levels can destabilize streambanks, and cause pop-out failures. This form of bank failure is caused by rapid changes in soil water content and cannot be predicted by the bank height-angle logistic regression analysis detailed in this report. Mitigating these erosive effects requires a combination of improved flow management and stream restoration to reconnect the channel to its floodplain.

Based on field observations and the data analysis described in this report, we can make some general recommendations for mitigating further channel instability in Big Dry Creek:

- **Flow management**: New and upgraded stormwater controls can mitigate the erosive power of high flows. This approach, however, shouldn't solely prioritize reducing peak flows. It is important to address both flow magnitude and duration to reduce cumulative stream power over time. Requiring full spectrum detention for new development will prevent further flow alteration and reduce the chance of additional channel erosion. Stormwater retrofits to existing development could also reduce erosion potential across the full range of flow events and further contribute to channel stability. Future work could more clearly define bank erosion thresholds (e.g. a maximum allowable discharge) that could be used as a design criteria for stormwater controls. In addition, irrigation releases from Standley Lake could potentially be managed to release the same volume of water over a longer time span, reducing flow peaks and flashiness; however, changing release patterns and/or timing is of course constrained by water rights administration and downstream uses.
- **Floodplain reconnection:** Reconnecting the stream to its floodplain can involve raising the channel bed or creating inset floodplains within the existing incised channel. This will allow high flows to dissipate energy on the floodplain, reducing their erosive power. In some areas, riparian vegetation is suffering because the channel is incised, lowering groundwater tables and reducing water availability for these plants. Floodplain reconnection will raise groundwater tables and improve riparian health. Much of the upper portion of Big Dry Creek flows through publicly-owned open space which makes this intensive restoration approach more feasible.
- **Grade control:** Although much of the channel appears relatively vertically stable, there is the potential for continued incision. This is primarily a concern in the lower portion of the watershed where there are fewer grade controls. While we observed some reaches with hardpan clay on the bed, it is unclear how thick these layers are and how long they will remain. Additionally, many areas show significant sand deposition, but these reaches may become erosion-dominated if sand supply from upstream decreases. Some preemptive grade control may be warranted in these areas to protect the channel against potential incision. Overlaying the bank stability and stream power data identified two sites with high transport capacity and banks near stability thresholds: just downstream from CR 21 and just downstream from CR 8 (reach 8A). See Map 5 for locations designated by arrows. Grade control structures in these areas can prevent further incision and could be designed to encourage sediment deposition, raising the channel bed and stabilizing the banks (Watson et al., 2002).

- **Bank stabilization/revegetation:** The GIS bank stability analysis (Maps 2 – 3) identified unstable banks. These data can be used to locate high-priority restoration areas (e.g. unstable sections near trails, roads, or other infrastructure) which may benefit from bank stabilization. Stabilization may entail grading banks to gentler slopes but should incorporate toe protection to avoid bank undercutting and failure. Additionally revegetation and other bioengineering techniques should be considered. The effectiveness of vegetation in preventing bank erosion was clearly seen during the field campaign (compare vegetated banks, photos 7 and 9, with unvegetated banks, photos 5, 6, and 8).
- **Monitoring and future analysis:** Whether or not stream restoration or stormwater management are implemented in Big Dry Creek, channel stability should be monitored in the future to identify potential channel changes – for example, renewed incision. A promising analysis method is DEM-differencing. This compares two DEMs from different times (e.g. the post 2013 flood DEM used in this analysis and a DEM collected at some future date) to identify erosion and deposition over that time period. This can identify areas in need of field reconnaissance and potentially more detailed analysis or modeling.

This report can be used to inform watershed and stream management to improve the health of Big Dry Creek. It is important, however, to consider watershed-scale effects when planning any management action. For example, stabilizing an eroding reach may improve the stream locally, but this could reduce sediment supply to a downstream reach and cause more erosion there. Addressing instability in Big Dry Creek holistically can improve this important community amenity and lead to a more resilient stream.

ACKNOWLEDGEMENTS

We wish to thank Urban Drainage and Flood Control District and the Big Dry Creek Watershed Association (specifically the City and County of Broomfield, City of Westminster, and Adams County) for providing funding for this work. Additional funding was provided by the United States Environmental Protection Agency (USEPA) grant RD835570. Its contents are solely the responsibility of the grantee and do not necessarily represent the official views of the USEPA. Further, USEPA does not endorse the purchase of any commercial products or services mentioned in the publication. We are also grateful to Jane Clary for sharing water quality data and her ongoing support for this project. Finally, we wish to thank Travis Hardee and Travis Stroth for assisting with the field work.

REFERENCES

Biron PM, Choné G, Buffin-Bélanger T, Demers S, Olsen T. 2013. Improvement of streams hydro-geomorphological assessment using LiDAR DEMs. *Earth Surface Processes and Landforms* **38**: 1808–1821.DOI: 10.1002/esp.3425.

NRCS. 2007. Stream Restoration Design. National Engineering Handbook, Part 654 210-VI-NEH

Schumm SA, Harvey MD, Watson CC. 1984. Incised Channels: Morphology, Dynamics and Control. Water Resources Publications: Littleton, CO

Watson CC, Biedenharn DS, Bledsoe BP. 2002. Use of incised channel evolution models in understanding rehabilitation alternatives. *Journal of the American Water Resources Association* **38**: 151–160.

PHOTOGRAPHS

Photo 1, Reach 1C: Looking upstream at a grade control structure in the upper part of Big Dry Creek. Note significant amount of rip-rap downstream from structure stabilizing the bed. This substrate also provides structure for filamentous algae growth.

Photo 2, Reach 2A: An eroding bank on the outside of a meander bend. In this section of Big Dry Creek, there is still significant coarser bed material. This coarse material makes up the majority of the bank toe while the upper bank is all sandy clay. View looking downstream.

Photo 3, Reach 2A: While there is evidence of bank erosion, the channel bed is relatively stable and even shows evidence of significant deposition (large bar on the right of the photo with coarse gravel/cobble and a finer sand patch). View looking upstream.

Photo 4, Reach 3B: View downstream of a large grade control structure stabilizes the channel bed in a park. Filamentous algae were abundant during the August field campaign, which was conducted during relatively low flow conditions.

Photo 5, Reach 3C: A tall, nearly vertical cutbank (~ 4.5 m or 15 ft). Sparse vegetation is doing little to stabilize this bank. Flow direction is left to right.

Photo 6, Reach 3C: A recent bank failure. Wetting-drying cycles appear to be weakening the bank material, making it more susceptible to fluvial erosion and mass failure. Flow direction is right to left.

Photo 7, Reach 4A: The outer bank of a meander bend stabilized by dense vegetation. View looking upstream.

Photo 8, Reach 4B: An unstable outer bank of a meander bend with no vegetation. View looking upstream.

Photo 9, Reach 5A: This reach appears to have been stabilized with rip-rap along the bank toes and possible willow plantings. The channel bed in this section is primarily stiff clay which may slow further incision. The lack of alluvium also suggests this reach has an excess of transport capacity. View looking downstream.

Photo 10, Reach 6A: Failed blocks of bank material temporarily protect the bank from further erosion. View looking downstream.

Photo 11, Reach 7A: A sandy, unstable bank with failed bank material. Banks in the lower reaches are generally shorter than in the upper watershed. View looking downstream.

Photo 12, Reach 8B: Evidence of deposition in the lower reaches of Big Dry Creek. In general, this lower section had much more sand than areas further upstream. Flow direction is left to right.

APPENDIX

Bank Phosphorus Data

This table includes the results of the bank phosphorus analysis. Three samples from one bank per site were collected and analyzed. Sample ID includes the site (e.g. 1A), bank (right or left), and the location of each sample (for each bank we sampled the bank toe, midway up the bank face, and near the top of the bank). In addition, one sample from clay bed material was included (5A-Bed2). Three methods for estimating phosphorus content were used. The EPA 3050a method is a measure of the total phosphorus content of the soil, including tightly bound phosphorus. The Mehlich 3 method is often used as an estimate of “bioavailable” phosphorus, or the phosphorus that is likely to be released from the soil and become available to biota. Water extractable phosphorus is simply the phosphorus that dissolves readily when the soil is placed in deionized water. In addition to phosphorus content, the soil texture was analyzed and reported.

Lab ID	Sample ID	EPA 3050a P	Mehlich 3 P	Water Extractable P	Sand	Silt	Clay	Texture
		----------mg/kg----------			----------%---------			
R2894	1A-RB-Toe	287	20.70	6.55	42	23	35	Clay Loam
R2895	1A-RB-Mid	283	16.36	5.65	52	15	33	Sandy Clay Loam
R2896	1A-RB-Top	368	34.38	15.00	38	21	41	Clay
R2897	1B-LB1-Toe	118	6.73	15.81	16	31	53	Clay
R2898	1B-LB1-Mid	346	14.44	16.10	31	21	48	Clay
R2899	1B-LB1-Top	460	38.62	36.28	35	19	46	Clay
R2900	1 C-LB-Toe	312	9.42	2.23	40	26	34	Clay Loam
R2901	1 C-LB-M id	379	22.82	6.88	50	16	34	Sandy Clay Loam
R2902	1 C-LB-Top	459	50.77	48.36	65	9	26	Sandy Clay Loam
R2903	2A-LB-Toe	323	21.86	15.60	68	10	22	Sandy Clay Loam
R2904	2A-LB-Mid	312	9.65	19.03	58	16	26	Sandy Clay Loam
R2905	2A-LB-Top	504	29.28	24.39	47	25	28	Sandy Clay Loam
R2906	2B-RB2-Toe	104	14.34	2.74	21	31	48	Clay
R2907	2B-R32-Mid	97	11.93	1.41	20	29	51	Clay
R2908	2B-R32-Top	134	30.53	11.1	43	9	48	Clay
R2909	2C-LB-Toe	373	5.86	4.32	73	6	21	Sandy Clay Loam
R2910	2C-LB-Mid	204	8.75	5.43	62	11	27	Sandy Clay Loam
R2911	2C-LB-Top	293	8.27	9.64	48	20	32	Sandy Clay Loam
R2912	3A-RB-Toe	189	9.52	31.95	78	1	21	Sandy Clay Loam
R2913	3A-RB-Mid	216	15.21	21.96	66	9	25	Sandy Clay Loam
R2914	3A-RB-Top	273	24.27	17.29	54	14	32	Sandy Clay Loam
R2915	3B-RB-Toe	360	21.18	9.59	59	17	24	Sandy Clay Loam
R2916	3B-RB-Mid	232	20.70	21.70	69	9	22	Sandy Clay Loam
R2917	3B-RB-Top	298	8.65	23.19	64	8	28	Sandy Clay Loam

Lab ID	Sample ID	EPA 3050a P	Mehlich 3 P	Water Extractable P	Sand	Silt	Clay	Texture
		----------mg/kg----------			----------%---------			
R2918	3C-LB-Toe	225	18.58	15.31	49	15	36	Sandy Clay
R2919	3C-LB-Mid	223	42.48	19.69	46	16	38	Sandy Clay
R2920	3C-LB-Top	183	18.58	30.76	66	8	26	Sandy Clay Loam
R2921	4A-RB-Toe	274	26.67	18.95	47	21	32	Sandy Clay Loam
R2922	4A-RB-Mid	228	23.49	30.99	7	34	59	Clay
R2923	4A-RB-Top	358	48.07	11.82	32	26	42	Clay
R2924	4B-LB-Toe	363	45.56	15.82	15	25	60	Clay
R2925	4B-LB-Mid	352	49.61	4.56	8	35	57	Clay
R2926	4B-LB-Top	342	48.45	14.71	46	18	36	Sandy Clay
R2927	4C-RB-Toe	339	17.90	9.01	38	23	39	Clay Loam
R2928	4C-RB-Mid	339	20.02	8.61	48	24	28	Sandy Clay Loam
R2929	4C-RB-Top	358	19.74	18.47	62	17	21	Sandy Clay Loam
R2930	5A-RB-Toe	307	17.13	24.15	63	18	19	Sandy Loam
R2931	5A-RB-Mid	360	33.13	33.81	40	28	32	Clay Loam
R2932	5A-RB-Top	341	55.78	34.70	50	21	29	Sandy Clay Loam
R2933	5B-RB-Toe	269	14.92	6.36	61	17	22	Sandy Clay Loam
R2934	5B-RB-Mid	309	30.24	19.24	66	16	18	Sandy Loam
R2935	5B-RB-Top	280	51.35	42.14	76	6	18	Sandy Loam
R2936	5C-LB-Toe	329	7.40	5.70	44	30	26	Loam
R2937	5C-LB-Mid	308	21.09	16.61	46	30	24	Loam
R2938	5C-LB-Top	240	45.37	35.41	78	4	18	Sandy Loam
R2939	6A-LB-Toe	241	17.33	10.23	66	13	21	Sandy Clay Loam
R2940	6A-LB-Mid	269	44.41	30.99	69	13	18	Sandy Loam
R2941	6A-LB-Top	377	56.16	37.05	62	19	19	Sandy Loam
R2942	6B-RB-Toe	303	46.91	12.13	32	26	42	Clay
R2943	6B-RB-Mid	392	50.19	17.73	14	37	49	Clay
R2944	6B-RB-Top	198	48.65	33.05	74	8	18	Sandy Loam
R2945	6C-RB-Toe	348	38.82	5.95	34	28	38	Clay Loam
R2946	6C-RB-Mid	285	41.71	12.28	52	18	30	Sandy Clay Loam
R2947	6C-RB-Top	447	81.99	8.93	42	20	38	Clay Loam
R2948	7A-RB-Toe	357	27.93	7.23	19	27	54	Clay
R2949	7A-RB-Mid	316	19.64	7.92	59	17	24	Sandy Clay Loam
R2950	7A-RB-Top	271	33.23	46.94	79	3	18	Sandy Loam
R2951	7B-RB-Toe	362	38.43	16.58	44	19	37	Clay Loam
R2952	7B-RB-Mid	841	258.3	55.25	54	16	30	Sandy Clay Loam
R2953	7B-RB-Top	584	186.1	141.9	49	23	28	Sandy Clay Loam
R2954	7C-RB-Toe	351	19.54	9.01	46	12	42	Sandy Clay

Lab ID	Sample ID	EPA 3050a P	Mehlich 3 P	Water Extractable P	Sand	Silt	Clay	Texture
		----------mg/kg----------			----------%---------			
R2955	7C-RB-Mid	268	12.03	3.31	34	25	41	Clay
R2956	7C-RB-Top	205	27.35	21.62	62	15	23	Sandy Clay Loam
R2957	8A-RB-Toe	159	26.48	13.85	46	20	34	Sandy Clay Loam
R2958	8A-RB-Mid	467	83.92	28.62	18	28	54	Clay
R2959	8A-RB-Top	439	64.26	4.79	19	42	39	Silty Clay Loam
R2960	8B-LB-Toe	246	37.66	30.03	79	4	17	Sandy Loam
R2961	8B-LB-Mid	215	41.13	32.60	72	10	18	Sandy Loam
R2962	8B-LB-Top	266	37.08	40.82	76	5	19	Sandy Loam
R2963	8C-RB-Toe	487	87.29	24.04	47	25	28	Sandy Clay Loam
R2964	8C-RB-Mid	562	133.1	37.91	42	29	29	Clay Loam
R2965	8C-RB-Top	449	79.58	36.46	59	19	22	Sandy Clay Loam
R2966	5A-Bed2	250	13.76	13.33	36	22	42	Clay